Detection and Location of Nonlinearities using Reciprocity Breakdown

IOP Conf. Series: Journal of Physics: Conf. Series **1106** (2018) 012028 doi:10.1088/1742-6596/1106/1/012028

Detection and Location of Nonlinearities using Reciprocity Breakdown

MG Wood[1,2], JET Penny[1] and MI Friswell[3]

[1] School of Engineering and Applied Science, Aston University, Birmingham B4 7ET, UK
[2] Mechanical Engineering, University of Sheffield, Sheffield S3 7QB, UK
[3] College of Engineering, Swansea University, Swansea SA1 8EN, UK

E-mail: j.e.t.penny@aston.ac.uk

Abstract. Damage in a structure often results in local stiffness nonlinearities and detecting these nonlinearities can be used to monitor the health of the structure. It is well-known that nonlinearities in structures lead to a breakdown in reciprocity, where the frequency response function between two points on the structure depends upon the forcing location. This paper proposes a measure to quantify the level of non-reciprocity in a structure and investigates the effect of the location and form of nonlinearity on this non-reciprocity measure. A simulated discrete mass-spring system was used to determine the effect of the excitation and response locations on the ability to detect the nonlinearity. Stepped-sine testing is commonly used to characterise a nonlinear system since harmonic excitation emphasises nonlinear phenomena and can, for example, allow the system to exhibit multiple solutions. Thus, a simulation of a stepped sine test was used as the benchmark to highlight reciprocity breakdown in the most favourable case. However, impact excitation is much easier and faster to implement in practice and consequently the effect of the type of excitation on the detection and location of nonlinearities was considered. Finally, the prospects for using a measure of reciprocity in a structural health monitoring system are discussed.

1. Introduction

Operational integrity is an essential requirement for any structure. Typically structures comprise an assembly of component parts, some of which may allow easy access to assess the robustness of those individual components through using either vision-based techniques or non-destructive examination methods [1, 2]. Conversely, some parts of a structure may not be accessible and a visual inspection or conventional non-destructive testing methods cannot be applied.

Safety critical structures range from composite aircraft skins and panels to concrete nuclear containments and so the aim of preventative maintenance is to identify damage within these structures as early as possible. In these cases, damage is most difficult to detect if it has occurred deep within a structure away from direct access for standard non-invasive assessment. Thus a great deal of research and innovation has centred upon identifying damage within continuous structures without the need for direct access [3].

Many approaches to damage location within structures involve the use of vibration in one form or another since its application is non-destructive [4]. In the case of safety critical structures, vibration based inspection is an approach that shows great promise [5]. Vibration testing provides a wealth of data and the interpretation of the data and the combination of outputs

proves most useful in damage location [6]. A number of authors have addressed the problem of quantifying the magnitude and location of damage within vibrating structures [7]. One approach to damage location using vibration is to use non-reciprocity as a measure [8, 9]; Manson *et al.* [10] provided an interpretation of non-reciprocity with a sound mathematical basis.

This paper investigates the non-reciprocal vibration outputs from an idealised discrete system that simulates damage by a simple nonlinear spring. A scalar based on the measured data between reciprocal locations is proposed to quantify the change of state (i.e. damage).

2. Non-Reciprocity

The vibration data from a structure or system under investigation is usually obtained experimentally to validate a mathematical model that represents its behaviour. Such mathematical models may be linearised to describe characteristics such as the natural frequencies, damping ratios and mode shapes [11]. Thus, in the practical case of periodic monitoring, any changes in these parameters should identify damage within a structure.

The principal vibrational signature of any structure or system obtained through vibration testing is the Frequency Response Function (FRF). A common type of FRF is the Inertance, $\mathbf{A}(\omega)$, given by

$$\mathbf{A}(\omega) = -\omega^2\alpha(\omega) = -\omega^2(\mathbf{K} - \omega^2\mathbf{M} + \imath\omega\mathbf{C})^{-1} \tag{1}$$

where $\mathbf{M}$, $\mathbf{K}$ and $\mathbf{C}$ are the mass, stiffness and damping matrices of the linearised system, and α is the Receptance. $A_{jk}(\omega)$ is the acceleration response at point j due to a unit harmonic excitation of frequency ω at point k, with no other forces being applied to the system. $A_{jk}(\omega)$ may also be expressed in terms of the natural frequencies and mode shapes; for modal damping the Inertance is

$$A_{jk}(\omega) = -\omega^2 \sum_{i=1}^{n} \frac{\{\boldsymbol{\phi}_i\}_j \{\boldsymbol{\phi}_i\}_k}{\omega_i^2 - \omega^2 + 2\imath\zeta_i\omega_i\omega} \tag{2}$$

where ω_i and ζ_i are the i th natural frequency and damping ratio, $\{\boldsymbol{\phi}_i\}_j$ and $\{\boldsymbol{\phi}_i\}_k$ are the j th and k th elements of the i th mode shape, and $\imath = \sqrt{-1}$.

An important characteristic of any linear structure is its reciprocal behaviour. Thus, if a structure is linear, then $A_{jk}(\omega)$ must equal $A_{kj}(\omega)$. However, the FRF can be affected by non-linearities in the structure and by the testing regime. For example, a system with a cubic-stiffness characteristic can exhibit a nonlinear response, such as softening or hardening behaviour, or jumps in the response, due to the type and level of excitation. From a purely physical perspective, regardless of the levels of care employed in their manufacture, all structures contain imperfections or flaws ranging from microscopic voids to material irregularities and both result in local nonlinearity. Subject to loading even within their operational envelopes, these structural voids and material irregularities become precursors of physical damage whereby repeated and / or cyclic loading propagate and magnify that damage using the original voids and irregularities as its source [12].

One measure of non-reciprocity may be expressed as the Difference of Reciprocity between degrees of freedom j and k (DoR_{jk}), where the absolute difference is averaged over the frequency range $[\omega_1, \omega_2]$, as

$$\mathrm{DoR}_{jk} = \int_{\omega_1}^{\omega_2} |A_{jk} - A_{kj}| d\omega \tag{3}$$

In order enhance this difference, the reciprocity may be normalised to give the Non Reciprocity Index (NRI_{jk}) as

$$\mathrm{NRI}_{jk} = 2\int_{\omega_1}^{\omega_2} |A_{jk} - A_{kj}|\, d\omega \Big/ \int_{\omega_1}^{\omega_2} |A_{jk}|+|A_{kj}|\, d\omega = 2\mathrm{DoR}_{jk} \Big/ \int_{\omega_1}^{\omega_2} |A_{jk}|+|A_{kj}|\, d\omega \tag{4}$$

The frequency range $[\omega_1, \omega_2]$ can either cover a whole frequency range of a test, or focus on specific resonances. In the examples used in this paper the DoR and NRI will be given for each resonance, since the effect of the location of the force and response degrees of freedom, and the location of the nonlinearity, will affect the non-reciprocity of each resonance differently.

The definitions of DoR and NRI in Eqs. (3) and (4) are given in terms of Inertance, as often acceleration is measured experimentally. However, Receptance or Mobility may be used, which will give a slightly different weight to the FRFs at each frequency; however this will have a limited influence on the conclusions from the DoR and NRI for each resonance as the frequency range will typically be small. Indeed the NRI values for small frequency ranges will be very similar for all types of FRFs because of the inherent normalisation.

3. Modal responses for weak nonlinearities

Damage is often local and the resulting nonlinearities are relatively weak. In this case the dynamics of the multi-degree-of-freedom system can be understood by transforming to the modes of the underlying linear system. This also helps to understand the magnitude of the differences (i.e. the DoR and DRI values) caused by the nonlinearity, as a function of the forcing location and the location of the nonlinearity. This can be demonstrated explicitly using a single cubic spring, but a similar analysis and conclusions could be undertaken for other nonlinearities.

Suppose a cubic spring is located between degrees of freedom r and s, then the equations of motion are

$$\mathbf{M}\ddot{\mathbf{q}} + \mathbf{C}\dot{\mathbf{q}} + \mathbf{K}\mathbf{q} + h\mathbf{t}x_c^3 = \mathbf{f}_0 f(t) \tag{5}$$

where $\mathbf{q}$ is the vector of generalised coordinates, h is the coefficient of the cubic spring and x_c is the relative displacement of this spring. In Eq. (5), vector $\mathbf{t}$ consists of zeros, except for 1 in position r and -1 in position s, and the vector $\mathbf{f}_0$ is a vector of zeros, with a 1 to select the excitation location.

Suppose now that the system is excited close to the i th natural frequency of the linear system, with the corresponding mode shape $\boldsymbol{\phi}_i$. Note that here we also assume light damping (or at least modal damping) and so $\boldsymbol{\phi}_i$ represents the real mass normalised mode shape of the undamped system. We will assume that the response is of the form

$$\mathbf{q}(t) = \boldsymbol{\phi}_i p_i(t) \tag{6}$$

where p_i is the scalar modal coordinate. This implies that degrees of freedom vibrate spatially as the mode shape, which will be only approximately true, even for weak nonlinearities. Transforming the equation of motion to the modal coordinate p_i gives

$$\ddot{p}_i + 2\zeta_i\omega_i\dot{p}_i + \omega_i^2 p_i + h\left(\boldsymbol{\phi}_i^\top \mathbf{t}\right) x_c^3 = \left(\boldsymbol{\phi}_i^\top \mathbf{f}_0\right) f(t) \tag{7}$$

The relative displacement of the cubic spring, x_c, can be expressed in terms of the vectors $\mathbf{t}$ and $\mathbf{q}$ thus:

$$x_c = \mathbf{t}^\top \mathbf{q} \tag{8}$$

Hence

$$x_c = \left(\mathbf{t}^\top \boldsymbol{\phi}_i\right) p_i = \left(\boldsymbol{\phi}_i^\top \mathbf{t}\right) p_i, \tag{9}$$

and Eq. (7) becomes

$$\ddot{p}_i + 2\zeta_i\omega_i\dot{p}_i + \omega_i^2 p_i + h\left(\boldsymbol{\phi}_i^\top \mathbf{t}\right)^4 p_i^3 = \left(\boldsymbol{\phi}_i^\top \mathbf{f}_0\right) f(t) \tag{10}$$

It is now clear how the different mode, force location and nonlinear spring location affects the nonlinear response. The modal force is given by $\left(\boldsymbol{\phi}_i^\top \mathbf{f}_0\right)$, which is not affected by the nonlinear

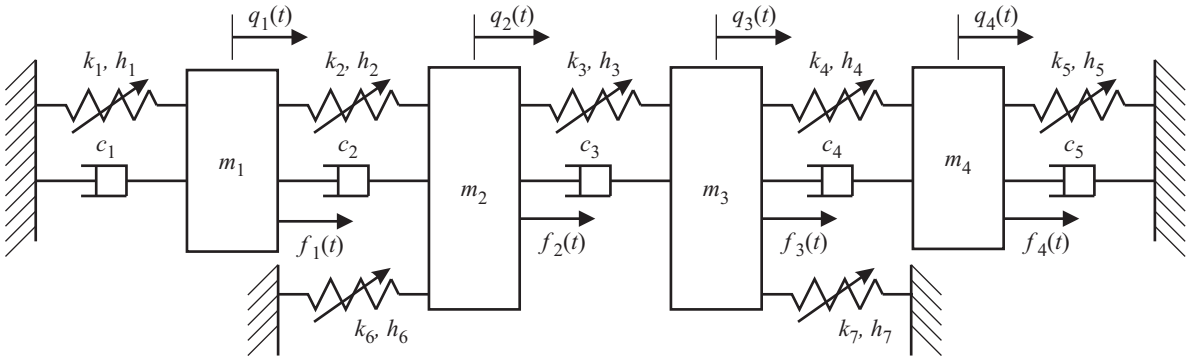

Figure 1. A schematic of the discrete four degrees of freedom system.

spring. The cubic spring coefficient is scaled by $\left(\boldsymbol{\phi}_i^{\top}\mathbf{t}\right)^4$, which depends on the mode shape of interest (i.e. the frequency of excitation) and the location of the nonlinearity. This will be explored further in the following examples.

4. Mass/spring example with stepped sine excitation

The lack of reciprocity, and its dependence on the locations of the excitation and nonlinearity, will now be demonstrated for a discrete mass-spring system with a cubic spring included selectively at a number of locations. The system is the four degree of freedom system shown in Figure 1, where k_i and h_i represent the linear and cubic coefficients for spring i. In all simulations the linear springs have stiffness $k_i = 1\,\text{kN/m}$ for $i = 1, \ldots, 5$ and $k_6 = k_7 = 0$. The discrete masses are $m_1 = 4\,\text{kg}$, $m_2 = 1\,\text{kg}$, $m_3 = 3\,\text{kg}$, and $m_4 = 2\,\text{kg}$. The natural frequencies of the linear system are 2.03, 3.39, 5.52 and 7.71 Hz, and discrete dampers are included to give damping ratios of 0.5% for all four modes. The mode shapes are

$$\boldsymbol{\phi}_1 = \begin{Bmatrix} 0.268 \\ 0.361 \\ 0.396 \\ 0.236 \end{Bmatrix}, \quad \boldsymbol{\phi}_2 = \begin{Bmatrix} 0.397 \\ 0.076 \\ -0.280 \\ -0.255 \end{Bmatrix}, \quad \boldsymbol{\phi}_3 = \begin{Bmatrix} 0.076 \\ -0.214 \\ -0.247 \\ 0.611 \end{Bmatrix}, \quad \boldsymbol{\phi}_4 = \begin{Bmatrix} -0.122 \\ 0.904 \\ -0.193 \\ 0.072 \end{Bmatrix}. \tag{11}$$

Only one cubic spring is simulated for each case, and hence only one of the h_i coefficients is non-zero. Table 1 shows the values of the equivalent modal constants for various locations of the nonlinear spring, and for the four modes. The values for the grounded springs are just the magnitude of the corresponding mode shapes element, and this also corresponds to the relative modal force for the excitation at this location. The table clearly shows that both the mode number and the location of the cubic spring will have a significant effect on the level of excitation of the nonlinearity.

4.1. Harmonic balance for sinusoidal excitation

The nonlinear system differential equations can be solved in the time domain using a standard numerical time stepping procedure such as the 4th order Runge-Kutta that simulates the experimental stepped sine test. However, here only the frequency domain information is required, and it is more efficient to use the harmonic balance (HB) method. In many cases, the HB method provides a faster method of solution although for a system producing a chaotic response this solution is not valid. The method assumes that the response of a system can be expressed as a truncated Fourier series, with a defined fundamental frequency ω_f. Should the response contain subharmonics then the excitation frequency, ω, will be an integer multiple of the response of the

Table 1. Modal constants for spring locations, $|\boldsymbol{\phi}_i^\top \mathbf{t}|$. A zero for the location indicates a grounded spring. Some cases do not correspond to a spring location given in Figure 1.

Spring Location	h_i	Mode 1	Mode 2	Mode 3	Mode 4
(1,2)	h_2	0.093	0.321	0.291	1.027
(2,3)	h_3	0.034	0.355	0.033	1.098
(3,4)	h_4	0.159	0.024	0.859	0.265
(1,3)		0.128	0.676	0.323	0.071
(2,4)		0.125	0.331	0.826	0.833
(1,4)		0.032	0.652	0.535	0.194
(0,1)	h_1	0.268	0.397	0.076	0.122
(0,2)	h_6	0.361	0.076	0.214	0.904
(0,3)	h_7	0.396	0.280	0.247	0.193
(0,4)	h_5	0.236	0.255	0.611	0.072

fundamental frequency ω_f. To solve a system using the HB method we substitute the truncated Fourier series for the response into the equations of motion, and the harmonic coefficients (either cosines / sines or complex exponentials) of the fundamental and harmonic frequencies lead to a set of nonlinear algebraic equations. For simple nonlinearities the well known trigonometric identities can be used to simplify the equations. Often this is not possible, and the Discrete Fourier Transform (DFT) is used to obtain the harmonic coefficients using the Alternating Frequency/Time (AFT) method [13].

4.2. FRFs and reciprocity for the example system

The initial example places a cubic spring between degrees of freedom 1 and 2; thus the nonlinear coefficients are $h_2 = 100\,\mathrm{N/m^3}$, and $h_i = 0$ for $i \neq 2$. A stepped sine test is performed with a force amplitude of 20 N, and the frequency is swept up from 1 Hz to 9 Hz with a frequency increment of 0.001 . The frequency is then swept back down to 1 Hz. Table 1 shows that mode 4 will show the strongest nonlinear effect, followed by modes 2 and 3 showing similar effects, and mode 1 showing a small effect. In terms of excitation, forcing at degree of freedom 2 will generate most force into mode 4, and forcing at degree of freedom 4 will produce the least force. Hence, Figure 2 compares the FRFs between degrees 2 and 4 (i.e. A_{24} and A_{42}) and both upward and downward frequency sweeps are plotted. It is clear that mode 4 shows a higher nonlinear response that the other modes, as expected. For A_{24}, the forcing level is low, and the response is near linear, with no jumps in the response. In contrast, or A_{42}, the forcing level is high, and the response shows a hardening behaviour and jumps in the response.

The DoR and NRI were calculated for these responses for each mode. The frequency bands used for each mode should be large enough to ensure that any nonlinear hardening or softening behaviour is captured, but small enough to ensure a single mode response is isolated. For this example a frequency bandwidth of 0.5 Hz is used, centred about the natural frequency of the linear system. The sweep up and sweep down are considered separately. Figures 3 and 4 show the calculated DoR and NRI and there is little difference between the up and down frequency sweeps. As expected, the DoR and NRI for mode 4 is most sensitive to the nonlinearity, and since the modal force amplitude for mode 4 is highest when the excitation is applied to degree of freedom 2, the DoR and NRI which include degree of freedom 2 are the highest. The conclusions from the DoR and NRI results are similar, but the NRI seems to give more emphasise to the nonlinear effects.

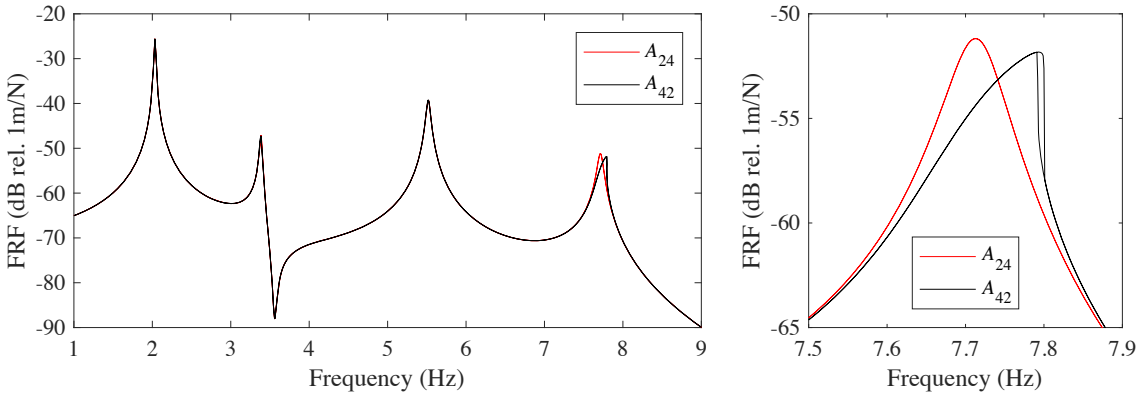

Figure 2. The FRFs between degrees of freedom 2 and 4, for both up and down frequency sweeps. The right plot is a zoom around mode 4.

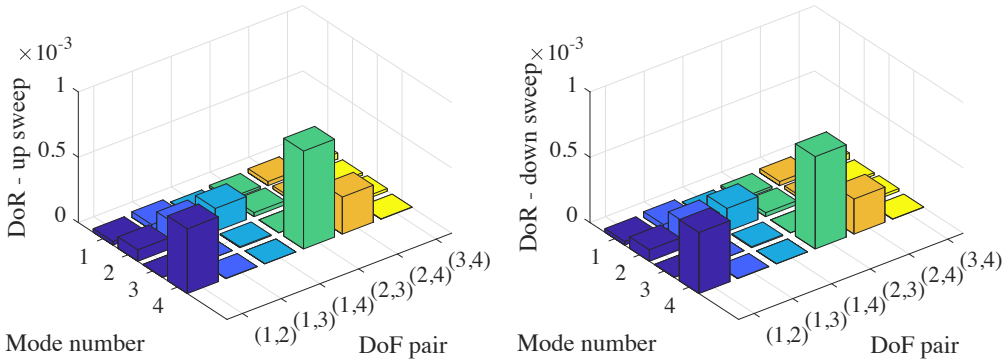

Figure 3. The Difference of Reciprocity for both up and down frequency sweeps.

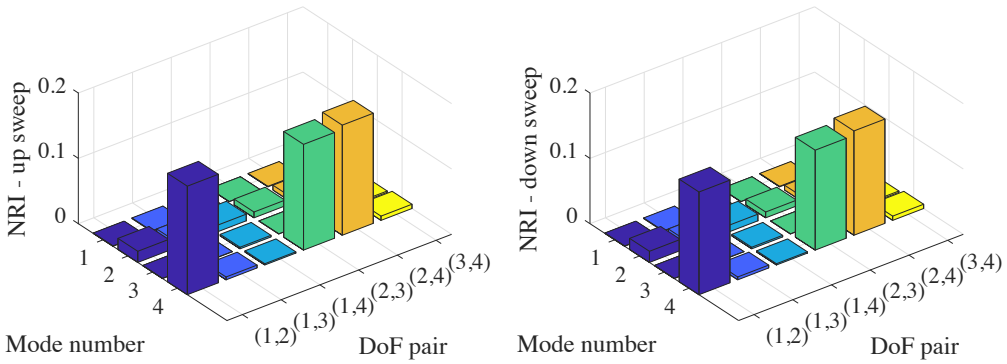

Figure 4. The Non Reciprocity Index for both up and down frequency sweeps.

The effect of force amplitude on $\mathrm{NRI}_{2,3}$ is shown in Figure 5 and, in this case, the NRI increases monotonically with the force amplitude. The amplitude of the NRI for mode 4 is highest, followed in order by modes 2, 1 and 3; from Table 1 it might be thought that mode 1 should have the lowest NRI, but the modal forcing and response obtained from the mode shapes, for degrees of freedom 2 and 3 are higher for mode 1 than mode 3.

A second example is now given for a grounded cubic spring at degree of freedom 2, i.e. $h_6 = 100\,\mathrm{N/m^3}$, and $h_i = 0$ for $i \neq 6$. Figure 6 shows the NRI for this case, and demonstrates

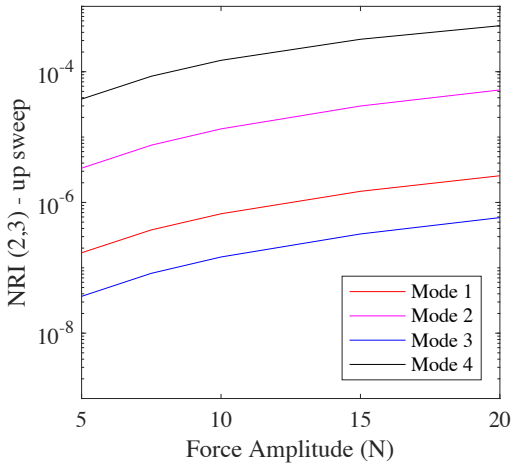

Figure 5. The Non Reciprocity Index $\mathrm{NRI}_{2,3}$ for a frequency up sweep.

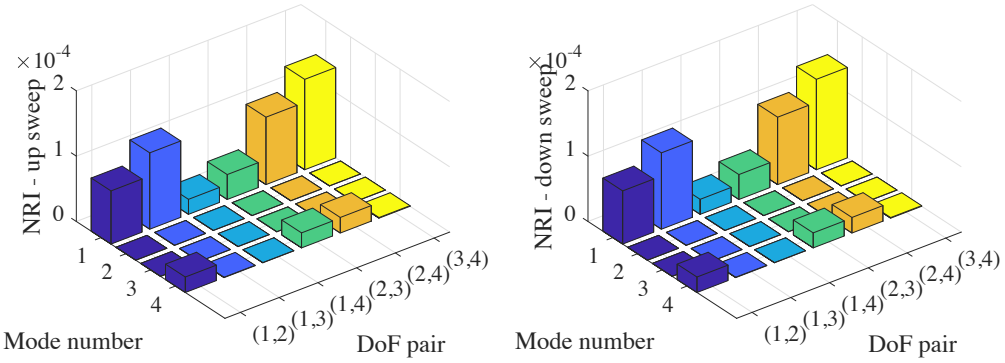

Figure 6. The Non Reciprocity Index for both up and down frequency sweeps for a grounded spring at DoF 2.

that modes 1 and 4 now have the highest NRI values. In this case mode 1 has the highest NRI values because of significantly higher modal excitation and response values.

5. Mass/spring example with impact excitation

A common excitation method is an impact force, and here this is modelled using a half sine pulse. The example used was the same 4 degrees of freedom mass-spring system used for the stepped sine testing with a cubic spring between degrees of freedom 1 and 2 with coefficient $h_2 = 100\,\mathrm{N/m^3}$, and $h_i = 0$ for $i \neq 2$. The impulse force has a peak amplitude of 2000 N and a duration of 25 ms. The response was simulated in the time domain using a 4th order Runge-Kutta algorithm and the FRF was obtained using the DFT. The DoR and NRI were obtained for each resonance, over a frequency range of 0.5 Hz centred about the linear natural frequencies, and the results are shown in Figure 7. The results are slightly different to those obtained from the stepped sine excitation, shown in Figures 3 and 4, but mode 4 is again the most sensitive to the nonlinearity and degree of freedom 2 also gives high NRI values.

6. Conclusions

Nonlinear multi-degree of freedom systems exhibit non-reciprocity in the measured FRFs, and the level of difference in the FRFs depends on the locations of the excitation, the response sensor,

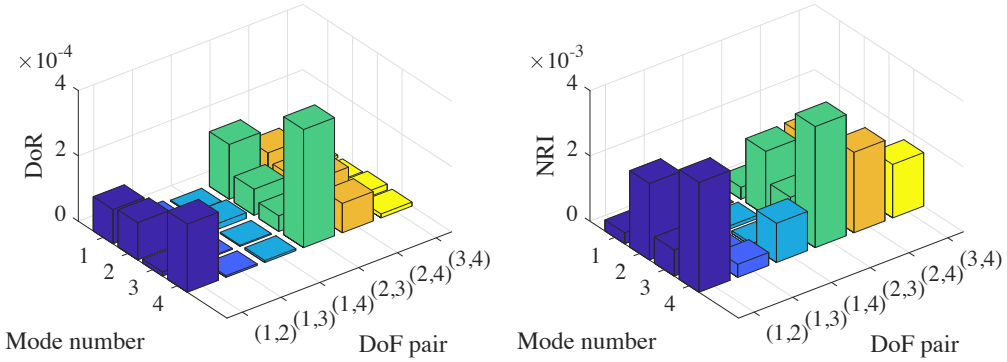

Figure 7. The Difference of Reciprocity and Non Reciprocity Index for impulse excitation.

and the localised nonlinearity. This paper has introduced two measures of non-reciprocity, the DoR and the NRI. A 4 degree of freedom mass-spring system has been used to demonstrate that the DoR and NRI are strongly dependent on the excitation of the nonlinearity, and for weak nonlinearities the linear mode shapes provide an efficient approach to understanding the resulting DoR and NRI values. In future this approach has the potential to efficiently determine the location of local nonlinearities in a structure.

7. References

[1] IAEA 2002 *Guidebook on Non-destructive Testing of Concrete Structures,* IAEA-TCS-17 Vienna, ISSN 10185518.

[2] Iliopoulos S, Aggelis D G, Pyl L, Vantomme J, Van Marcke P, Coppens E & Areias L 2015 Detection and evaluation of cracks in the concrete buffer of the Belgian nuclear waste container using combined NDT techniques, *Construction and Building Materials* **78** 369-78.

[3] Doebling S W, Farrar C R, Prime M B & Shevitz D W 1996 Damage identification and health monitoring of structural and mechanical systems from changes in their vibrational characteristics: a literature review, *Los Alamos National Laboratory,* New Mexico, Report LA-13070-MS

[4] Klepka A, Straczkiewicz M, Pieczonka L, Staszewski W J, Gelman L, Aymerich F & Uhl T 2015 Triple correlation for detection of damage-related nonlinearities in composite structures, *Nonlinear Dynamics* **81** 453-68.

[5] Zwink B R, Adams D E, Evans R D & Koester D J 2009 Wide-area damage detection in military composite helicopter structures using vibration-based reciprocity measurements, *Proc of the IMAC-XXVII,* 9-12 February 2009, Orlando, Florida USA.

[6] Rogers T, Manson G & Worden K 2016 On the behaviour of structures with many nonlinear elements, ed. De Clerck J & Epp D (eds) Rotating Machinery, Hybrid Test Methods, Vibro-Acoustics & Laser Vibrometry **8** *Proc of the Society for Experimental Mechanics Series* Springer, Cham.

[7] Chesne S & Deraemaeker A 2013 Damage localization using transmissibility functions: A critical review, *Mechanical Systems and Signal Processing* **38** 569-84.

[8] Wood M G, Penny J E T, Purkiss J A, Short N R & Owolawi O 2003 Measuring changes of state in concrete, *Materials Science Forum* **440-1**, 219-28

[9] Wood M G 1992 *Damage Analysis of Bridge Structures using Vibrational Techniques*, PhD Thesis, University of Aston, Birmingham, UK.

[10] Manson G, Worden K & Wood M G 2012 Analysis of reciprocity breakdown in nonlinear systems, *Proc Modern Practice in Stress and Vibration Analysis,* University of Glasgow, 31 August 2012, IoP Press.

[11] Gloth G & Sinapius M 2005 Analysis of swept-sine runs during modal survey and qualification tests, *Proc of the European Conference on Spacecraft Structures, Materials and Mechanical Testing* 10-12 May 2005, ESA SP-581 Noordwijk, The Netherlands.

[12] Patrício M 2008 *Crack Propagation on Highly Heterogeneous Composite Materials*, PhD Thesis, Eindhoven University of Technology, The Netherlands.

[13] Cameron T M & Griffin J H 1989 An alternating frequency/time domain method for calculating the steady-state response of nonlinear dynamic systems, *Journal of Applied Mechanics* **56** 149-154.